Tumor-intrinsic PD-L1 signals regulate cell growth, pathogenesis and autophagy in ovarian cancer and melanoma

Clark, Curtis A.; Gupta, Harshita B.; Sareddy, Gangadhara; Pandeswara, Srilakshmi; Lao, Shunhua; Yuan, Bin; Drerup, Justin M.; Padron, Alvaro; Conejo-Garcia, Jose; Murthy, Kruthi

Published in:
Cancer Research

DOI:
10.1158/0008-5472.CAN-16-0258

Publication date:
2016

HHS Public Access

Author manuscript

Cancer Res. Author manuscript; available in PMC 2017 December 01.

Published in final edited form as:

Cancer Res. 2016 December 01; 76(23): 6964–6974. doi:10.1158/0008-5472.CAN-16-0258.

Tumor-intrinsic PD-L1 signals regulate cell growth, pathogenesis and autophagy in ovarian cancer and melanoma

Curtis A. Clark[1,2], **Harshita B. Gupta**[2], **Gangadhara Sareddy**[4,9], **Srilakshmi Pandeswara**[2], **Shunhua Lao**[2], **Bin Yuan**[2,5], **Justin M. Drerup**[1,2], **Alvaro Padron**[2], **José Conejo-Garcia**[6], **Kruthi Murthy**[1,2], **Yang Liu**[2,3], **Mary Jo Turk**[7], **Kathrin Thedieck**[8], **Vincent Hurez**[2], **Rong Li**[1,4,5], **Ratna Vadlamudi**[1,4,9], and **Tyler J. Curiel**[1,2,4,*]

[1]The Graduate School of Biomedical Sciences, University of Texas Health Science Center, San Antonio, TX 78229

[2]Department of Medicine, University of Texas Health Science Center, San Antonio, TX 78229

[3]Xiangya School of Medicine, Central South University, Changsha, Hunan 410013, P.R. China

[4]Cancer Therapy & Research Center, University of Texas Health Science Center, San Antonio, TX 78229

[5]Department of Molecular Medicine, University of Texas Health Science Center, San Antonio, TX 78245

[6]Tumor Microenvironment and Metastasis Program, The Wistar Institute, Philadelphia, PA 19104

[7]Department of Microbiology and Immunology, Geisel School of Medicine at Dartmouth, Hanover, New Hampshire 03755

[8]Department of Pediatrics, Center for Liver, Digestive and Metabolic Diseases, University of Groningen, University Medical Center Groningen, 9713 AV Groningen, The Netherlands and Department for Neuroscience, School of Medicine and Health Sciences, University Oldenburg, 26129 Oldenburg, Germany

[9]Department of Obstetrics and Gynecology, University of Texas Health Science Center, San Antonio, TX 78229

Abstract

PD-L1 antibodies produce efficacious clinical responses in diverse human cancers, but the basis for their effects remains unclear, leaving a gap in understanding of how to rationally leverage the therapeutic activity. PD-L1 is widely expressed in tumor cells but its contributions to tumor pathogenicity are incompletely understood. In this study, we evaluated the hypothesis that PD-L1 exerts tumor cell-intrinsic signals that are critical for pathogenesis. Using RNAi methodology, we attenuated PD-L1 in the murine ovarian cell line ID8agg and the melanoma cell line B16 (termed PD-L1lo cells), which express basal PD-L1. We observed that PD-L1lo cells proliferated more

*To whom correspondence should be addressed: Tyler Curiel, MD, MPH, Department of Medicine, University of Texas Health Science Center at San Antonio, STRF MC 8252, 8403 Floyd Curl Drive, San Antonio, TX 78229-3900, USA. Phone: 210-562-4083, curielt@uthscsa.edu.

Competing interests: The authors have no conflicting financial interests to declare.

weakly than control cells in vitro. As expected, PD-L1lo cells formed tumors in immunocompetent mice relatively more slowly, but unexpectedly, they also formed tumors more slowly in immunodeficient NSG mice. A comparative microarray analysis identified a number of genes involved in autophagy and mTOR signaling that were affected by PD-L1 expression. In support of a functional role, PD-L1 attenuation augmented autophagy and blunted the ability of autophagy inhibitors to limit proliferation in vitro and in vivo in NSG mice. PD-L1 attenuation also elevated mTORC1 activity and augmented the anti-proliferative effects of the mTORC1 inhibitor rapamycin. PD-L1 cells were also relatively deficient in metastasis to the lung and we found that anti-PD-L1 administration could block tumor cell growth and metastasis in NSG mice. This therapeutic effect was observed with B16 cells but not ID8agg cells, illustrating tumor- or tissue-specific effects in the therapeutic setting. Overall, our findings extend understanding of PD-L1 functions, illustrate non-immune effects of anti-PD-L1 immunotherapy and suggest broader uses for PD-L1 as a biomarker for assessing cancer therapeutic responses.

Keywords

PD-L1; B7-H1; PD-1; mTOR; autophagy; ovarian cancer; melanoma; human

Introduction

PD-L1 (B7-H1, CD274), an immune co-signaling molecule in the B7-H (B7 homology) family (1), negatively regulates T cell functions through PD-1 and CD80 interactions (2), and is immunopathogenic in diverse cancers (3). Anti-PD-L1 monoclonal antibodies (αPD-L1) are clinical efficacy against distinct cancers where the principal mechanism of action is thought to be protecting PD-1-expressing anti-tumor T cells from inhibition by tumor PD-L1 (3–7). αPD-L1 is FDA-approved for bladder cancer. αPD-1 was recently FDA-approved to treat melanoma, renal cell carcinoma, non-small cell lung cancer and head and neck cancers. It is also proposed to work by protecting PD-1-expressing anti-tumor T cells from inhibition by tumor surface-expressed PD-L1, among other potential mechanisms (7,8).

Because of the promise of αPD-L1 and αPD-1 immunotherapy, much attention has focused on effects of the tumor PD-L1/T cell PD-1 axis in cancer immunotherapy and immunopathogenesis. Following the initial report that tumor PD-L1 kills anti-tumor T cells (4), most work on PD-L1 signals in cancer has focused on tumor-extrinsic PD-L1 effects, particularly on T cells. However, recent work shows that tumor PD-L1 prevents tumor apoptosis (9), reduces chemotherapy-mediated killing by altering mitogen activated protein kinase signals (10) and regulates tumor glucose metabolism in sarcomas (11). Thus, tumor PD-L1 has important tumor-intrinsic signaling and survival effects, but these are little studied.

In our studies of αPD-L1 immunotherapy we used RNAi technology to engineer low PD-L1-expressing tumors cells (termed PD-L1^{lo}) from parental PD-L1-expressing cell lines and made the unexpected observation that PD-L1^{lo} tumor cells proliferated more slowly than control cells *in vitro*, prompting us to study tumor-intrinsic PD-L1 signaling effects in more detail. We found that tumor PD-L1 had profound effects on expression of many genes that

play important roles in tumor signaling and metabolism, including mammalian target of rapamycin (mTOR) and autophagy pathways. Autophagy is a catabolic mechanism utilized by tumor cells to modulate cellular stress and metabolism, and is targeted to treat some cancers (12). We demonstrated that αPD-L1 antibody used as immunotherapy had unexpected, important tumor-specific effects on tumor growth and metastatic spread, and that tumor PD-L1 also affected sensitivity to pharmacologic autophagy and mTOR inhibitors and cytokines. These data shift the current paradigm regarding the role of PD-L1 effects on tumor immunopathogenesis and response to immune checkpoint blockade inhibitory antibodies to include tumor-intrinsic signaling consequences, suggest approaches to treatment based on tumor PD-L1 status in novel ways and suggest that PD-L1 could be a biomarker for treatments other than αPD-L1 or αPD-1.

PD-1, PD-L1 and B7-H3 are all immunoglobulin superfamily members (13), and all regulate tumor mTOR (14,15) (and our new data here). Thus, this superfamily appears to have common tumor cell-intrinsic effects on important cell signaling and functional outcomes that require much additional study. Our work demonstrates additional tumor-intrinsic effects in this superfamily, with a focus on PD-L1.

Materials and Methods

Mice

Wild type (WT) C57BL/6J (BL6), βδ TCR knockout (KO), and NOD.Cg-Prkdc^{scid}Il2rg^{tm1Wj1}/SzJ (non-obese diabetic/severe combined immunodeficiency (NOD/SCID)/interleukin (IL)-2Rγ KO, NSG) mice were purchased from Jackson Laboratory. PD-L1 KO mice were a kind gift from Lieping Chen (16). All mice were syngeneic BL6 and maintained under specific pathogen free conditions and given food and water *ad libitum*. Age- and sex-matched mice that were at least 8 weeks of age were used for all experiments. Only females were used for ID8agg ovarian cancer studies. All animal studies were approved by The University of Texas Health Science Center at San Antonio Institutional Animal Care and Use Committee.

In vivo tumor challenges, treatments and assessments

Tumor challenge into all mice except NSG was injection of 5 x 10^5 B16 cells subcutaneously as described (16), or 4 x 10^6 ID8agg cells intraperitoneally. For NSG mice, 1.5 x 10^5 B16 or 1 x 10^6 ID8agg cell challenges were used. B16 growth was measured every other day with Vernier calipers and volume calculated as (length x width^2)/2. Survival was determined as tumor >1500 mm^3 or distress (16). ID8agg tumor burden was determined by *in vivo* luciferase imaging and survival was assessed by ascites formation, weight gain or distress (17).

αPD-L1 (10F.9G2) and αPD-1 (RMP1-14) antibodies or respective isotype controls were injected intraperitoneally. In NSG mouse challenges, we gave 200 μg/mouse every other day starting 1 day before tumor challenge. In WT challenge we gave 100 μg/mouse αPD-L1 or isotype control every 5 days for B16 or ID8agg cell starting on day 7 after tumor challenge for times indicated.

For pharmacologic autophagy inhibition *in vivo*, mice were injected intraperitoneally with chloroquine 60 mg/kg every other day (18,19) or 3-methyladenine 25 mg/kg every 5 days (20) versus PBS control starting on day 7 following tumor challenge, regimens shown to inhibit tumor cell autophagy effectively *in vivo*.

In vivo luciferase detection was performed on an IVIS Lumina (Perkin-Elmer) with isoflurane-anaesthetized mice 15 minutes after intraperitoneal injection with 200 μL luciferin potassium (15 mg/mL, Gold Biotechnology) with a 30 second exposure. An identical region of interest was drawn over each abdomen and tumor burden was quantified as average radiance (photons/second/cm^2/sr).

Cell lines and transfections

Mouse B16-F10 melanoma (herein “B16” for simplicity) and ID8 ovarian cancer, and human ES2 ovarian cancer cells were purchased from the American Type Culture Collection. Cells were not revalidated for this work. We generated an aggressive ID8 line, ID8agg, by serial passage through WT hosts (Suppl. Fig. 1). Mouse cells were used in passages <5 and ES2 was passaged for <6 months. All cells were maintained in 5% fetal bovine serum (FBS)-containing RPMI-1640 medium supplemented with 1% penicillin/streptomycin, 1% L-glutamate, and 1% HEPES buffer. For serum starvation experiments, 0.1% FBS replaced 5.0%.

Stable PD-L1 knockdown in B16 and ID8agg lines was generated using lentivirus transduction particles containing validated PD-L1 shRNA (Sigma, TRCN0000068001) against murine *Pdcd1lg1* in pLKO.1-puro vector using puromycin selection per manufacturer’s protocol (Suppl. Fig. 2C). Scrambled PD-L1 shRNA control sequence (Sigma, SHC216V) was used to generate control lines. Individual PD-$L1^{lo}$ clones were selected in 2 μg/ml puromycin. For ES2, PD-L1 shRNA (Sigma, TRCN0000056914) against human *Pdcd1lg1* and controls were used as described above. Individual PD-$L1^{lo}$ clones were selected in 4 μg/ml puromycin. The PD-L1-overexpressing (PD-$L1^{hi}$) B16 polyclonal line was generated by transfection of pCMV6-PD-L1-GFP plasmid (OriGene, MG203953) using Turbofect (ThermoFisher) per the manufacturer’s protocol (Suppl. Fig. 2D). Pooled PD-$L1^{hi}$ clones stably expressing PD-L1-GFP were obtained using G418 selection. Luciferase expression was engineered into ID8agg cells by transfection with pGL4.51 [luc2/CMV/neo] plasmid DNA (Promega) and Attractene transfection reagent (Promega) according to manufacturer instructions and individual clones were selected with G418.

Flow cytometry

Cells were stained and sorted as previously described (21), using LSR II and FACSAria hardware and analyzed by FACSDiva (BD Bioscience) and FlowJo software (FlowJo, LLC). Anti-mouse PD-L1 (10F.9G2), anti-mouse PD-1 (29F.1A12) and matched isotype control antibodies were purchased from BioLegend. Cells were treated with recombinant mouse interferon (IFN)-γ (0.1 ng/mL, R&D Systems) for 48 hours as noted to induce PD-L1.

In vitro cell proliferation

Cells (6 x 10^3) were plated in 96-well plastic culture plates in medium and treated 12 hours later with chloroquine (50 μM), 3-methyladenine (5 mM), rapamycin (5 nM) (Sigma for all), TNF-α (10 ng/mL; R&D Systems), cisplatin (Sigma; 1–10 μM), or paclitaxel (Sigma; 1–30 nM). αPD-L1 (10F.9G2) or αPD-1 (RMP1–14) antibodies or respective isotype controls were used at 50 μg/mL for the entire culture period. Data shown are from optimized drug concentrations in preliminary work not shown. Cell proliferation rates were determined using MTT (3-(4, 5-dimethylthiazolyl-2)-2, 5-diphenyltetrazolium bromide, 5 mg/mL), which measures metabolic activity, 72 h after treatment. Absorbance was measured at 540 nM using a BioTek Synergy 2 Multi-Mode Plate Reader (Winooski, VT). Data are presented as mean absorbance versus medium control ± standard error of the mean (SEM). Proliferation was assessed in triplicate and compiled from three separate experiments. Cell viability was determined using a Vi-Cell XR (Beckman Coulter).

RNA sequencing (RNA-seq)

Total RNA was isolated from control ID8agg and ID8agg PD-$L1^{lo}$ (clone 3) cells using RNeasy (Qiagen), and RNA quality was ensured on an Agilent Bioanalyzer. 50 base pair single read sequencing was performed using an Illumina HiSeq 2000 system at The UTHSCSA Genome Sequencing Facility. Data are presented as gene sequence fold-change in PD-$L1^{lo}$ versus control. RNA-seq data was also analyzed by DAVID Bioinformatics and corrected for multiple comparisons. Genomic data will be deposited in the Gene Expression Omnibus database.

Immunoblotting

Cell lysates were prepared in RIPA buffer (20 mM Tris–HCl pH 8.0, 150 mM NaCl, 1 mM disodium EDTA, 1 mM EGTA, 2.5 mM sodium pyrophosphate, 1 mM β-glycerophosphate, 1% triton-X100) plus 1 mM phenylmethylsulphonyl fluoride and Halt protease/phosphatase inhibitor cocktail (Thermo Scientific). Protein concentration was measured by Bradford method (Thermo Scientific). 50 μg protein was separated by 4–15% sodium dodecyl sulfate polyacrylamide gels (BioRad Hercules), transferred to PVDF membranes (GE Water and Process Technologies), blocked in Tris-buffered saline (pH 7.4) plus 0.1% Tween-20 and 5% skim milk, and incubated overnight at 4° C with 1:1000 diluted phospho- and/or total antibodies against indicated proteins (Cell Signaling) plus anti-mouse β-actin (Santa Cruz Biotechnology). Membranes were incubated with horse radish peroxide-conjugated antibodies, 1 h. Proteins were detected by enhanced chemiluminescence (Pierce). Band quantification and normalization to total protein was by ImageJ software (22). Data show means of 3 individual blots with comparisons only made between like blots from the same gels.

Microscopy

Cells were plated at low confluence in 6 well plates (50,000 cells/well). On day 2, cells were exposed to serum starvation (0% FBS), normal medium (10% FBS), or chloroquine (50 μM) for 24 hours. Medium was removed, cells were washed with PBS and treated with 4% paraformaldehyde/PBS for 20 minutes at room temperature, washed, then permeabilized

with 0.1% Triton X-100 for 10 minutes. Cells were then blocked with 5% normal goat serum (Cell Signaling Technology) containing 0.3% Triton X-100 in PBS for 60 minutes. Diluted primary antibody, anti-mouse LC3 A/B (Cell Signaling Technology), was applied in blocking buffer overnight at 4° C. Alexa Fluor-555 secondary antibody diluted in 1% normal goat serum in PBS were added for 1 hour at ambient temperature. Cells were fixed using Vectashield hard set mounting medium containing DAPI dye (Vector Laboratories). Images were acquired using confocal microscopy (Olympus FV-1000) and overlaid using ImageJ (22).

Quantitative RT-PCR

Total RNA was isolated from homogenized whole lung tissue using RNeasy (Qiagen). cDNA was synthesized with 1 μg of total RNA using the ImPromII Reverse Transcription System (Promega) and random primers. Quantitative PCR (qPCR) was conducted using the 7900HT Real-Time PCR System (Applied Biosystems), amplified with transcript-specific primers with SYBR Green (Thermo Scientific), according to manufacturer's instructions. Mouse primers were: *Tyr*, 5′-CTCTGGGCTTAGCAGTAGGC-3′ and 5′-GCAAGCTGTGGTAGTCGTCT-3′; *gp100*, 5′-ACATTTCATCACCAGCAGGGTGCC-3′ and 5′-AACAAGTGGGTGCTGGCC-3′; *Trp-2*, 5′-GTCCTCCACTCTTTTACAGACG-3′ and 5′-ATTCGGTTGTGACCAATGGGT; *Trp-1*, 5′ CCCCTAGCCTATATCTCCCTTTT-3′ and 5′-TACCATCGTGGGGATAATGGC-3′; and *Gapdh*, 5′-AACGACCCCTTCATTGAC-3′ and 5′-TCCACGACATACTCAGCAC-3′ as the internal control (23).

Statistical analysis

Statistical analyses were conducted with Prizm software (GraphPad). Data in bar graphs are means ± SEM. For tumor growth, we used two-way ANOVA plus Bonferroni post-tests to compare replicate means. Kaplan-Meier estimates and the log-rank test were used to analyze statistical differences in survival. For all other single measurement assays, we used an unpaired *t* test. $P<0.05$ was considered significant.

Results

ID8agg and B16 express inducible PD-L1

The ID8 ovarian cancer cell line produces tumors that replicate important aspects of human disease, including local spread and ascites after intraperitoneal injection into syngeneic BL6 mice (24) but disease is not manifest for 10–15 weeks (16). We generated an aggressive ID8 line, ID8agg, by serial passage through WT hosts that produces rapid disease (Suppl. Fig. 1). Flow cytometry showed that ID8agg cells express PD-L1 that is upregulated by IFN-γ (Fig. 1A), and immunoblot and confocal microscopy confirmed PD-L1 expression (Suppl. Fig. 2A). B16 melanoma cells also express basal PD-L1 that is further upregulated by IFN-γ (Fig. 1B, Suppl. Fig. 2B).

Tumor intrinsic PD-L1 regulates ID8agg and B16 cell proliferation *in vitro* and *in vivo*

We used plasmids stably expressing shRNA to reduce basal and IFN-γ-inducible PD-L1 expression (PD-L1^{lo}) in ID8agg and B16 cells, and a constitutively active vector to increase

PD-L1 expression in B16 (PD-L1^{hi}, Fig. 1A,B, Suppl. Fig. 2). PD-L1^{lo} B16 cells proliferated significantly slower than control B16 cells and PD-L1^{hi} cells exhibited the highest rate of proliferation *in vitro* (Fig. 1C). Subcutaneous WT mouse challenge elicited a similar trend, with PD-L1^{hi} B16 cells producing the fastest tumor growth and PD-L1^{lo} cells the slowest (not shown). Tumor PD-L1 can inhibit anti-tumor immunity by impeding anti-tumor CD8^{+} T cell function (4). Thus, to dissect tumor cell-intrinsic effects versus immune effects *in vivo*, we challenged severely immune-deficient NSG mice with distinct B16 cell constructs subcutaneously. Consistent with *in vitro* and WT challenge data, in the absence of tumor-specific immunity, PD-L1^{hi} B16 tumors grew fastest and PD-L1^{lo} tumors grew the slowest (Fig. 1D, left), which correlated with reduced overall survival (Fig. 1D, right). Further, PD-L1^{hi} cells generated the greatest lung metastases following subcutaneous challenge whereas PD-L1^{lo} cells produced the fewest as detected by PCR for tumor-specific gene products (Fig. 1E). In support, PD-L1^{lo} ID8agg cells grew more slowly *in vitro* (Fig. 1F), and *in vivo* compared to control ID8agg after intraperitoneal challenge in WT (not shown) and NSG mice (Fig. 1G). Together, these data clearly demonstrate that tumor intrinsic PD-L1 controls tumor growth *in vitro* and *in vivo* in distinct tumors and anatomic compartments. PD-L1-mediated growth and promotion of *bona fide* metastatic tumor spread were all independent of anti-tumor immunity.

αPD-L1 retards B16 but not ID8agg tumor growth in NSG mice

To determine if tumor cell proliferation rate is influenced by PD-L1 or PD-1 surface expression, we first showed that B16 also expresses PD-1 as reported (15) and found that ID8agg also expresses PD-1 (Fig. 2A). Proliferation of control but not PD-L1^{lo} B16 cells *in vitro* was significantly reduced by both αPD-L1 and αPD-1 (Fig. 2B). CD80 was not detected (not shown). To assess if αPD-L1 reduces tumor growth in mice lacking anti-tumor immunity, we challenged NSG mice with control B16 cells and treated with αPD-L1, which reduced control B16 (Fig. 2C) and PD-L1^{hi} B16 growth (Suppl. Fig. 3A), consistent with *in vitro* data. We confirmed that αPD-1 slows control B16 growth in NSG mice (not shown) as reported (15). To determine the role of tumor cell-intrinsic PD-L1 in metastatic propensity, primary lung metastases in NSG mice challenged subcutaneously with B16 were assessed as mRNA of melanoma-specific genes in lung homogenates as described (23). αPD-L1 or αPD-1 each reduced B16 lung metastases significantly and similarly (Fig. 2D, Suppl. Fig. 3B). Similar to B16, αPD-L1 and αPD-1 each reduced rates of control ID8agg cell proliferation *in vitro*, but without significant effect on PD-L1^{lo} ID8agg (Fig. 2E). By contrast, αPD-L1 had negligible treatment effects on peritoneal ID8agg cell challenge into WT mice (Suppl. Fig. 4), and did not slow tumor growth or improve survival in NSG challenge (Fig. 2F,G). Thus, whereas certain PD-L1 signaling effects are similar in distinct tumors (and see data to follow), αPD-L1 effects *in vivo* can be dissociated from *in vitro* effects, as well as from PD-L1 effects in distinct tumors as also seen in lack of αPD-L1 effects on PD-L1-expressing sarcoma growth in NSG mice (11).

Tumor PD-L1 is the target of αPD-L1-mediated B16 growth inhibition

It is possible that αPD-L1 acts on host PD-L1 to mediate tumor growth inhibition. We first showed that αPD-L1 treated control B16, but not PD-L1^{lo} B16 in wild type mice (Suppl. Fig. 5A,B). To assess host PD-L1 effects specifically, we showed that αPD-L1 treated

parental B16 challenge into PD-L1 KO mice as effectively as in wild type mice, whereas αPD-L1 had no effect on PD-L1^{lo} B16 challenge in PD-L1 KO mice (Suppl. Fig. 5C,D). Therefore, tumor PD-L1 expression is necessary and sufficient for αPD-L1 effects on B16 growth *in vivo,* and host PD-L1 is not required, consistent with anti-proliferative effects *in vitro* (Fig. 2B).

PD-L1 alters tumor-intrinsic signaling

Data thus far clearly indicate a major cell-intrinsic, immune-independent role for tumor PD-L1 in both ovarian cancer and melanoma cells. We next investigated PD-L1-dependent signaling pathways. RNA-seq of control versus PD-L1^{lo} ID8agg cells identified 1269 differentially expressed basal genes using a 2-fold change cutoff (Fig. 3A and data not shown), including significant gene expression differences in canonical and non-canonical autophagy pathways (Table 1, top).

Tumor PD-L1 regulates autophagy

We assessed PD-L1 effects on autophagic flux as conversion of LC3-I to LC3-II in parental ID8agg or PD-L1^{lo} cells. Serum starvation for 24 hours augmented autophagy in control cells as expected. Autophagic flux was significantly higher in basal PD-L1^{lo} versus control ID8agg cells as assessed by LC3-II/LC3-I ratio (25) but serum starvation did not increase LC3-II further in PD-L1^{lo} cells (Fig. 3B) suggesting that tumor PD-L1 regulates basal and starvation-induced autophagy in ID8agg. In support of PD-L1-mediated autophagy suppression, LC3 foci formation was lower in control versus PD-L1^{lo} ID8agg (Fig. 3C). PD-L1 also blunted basal autophagic flux in B16, but in contrast to ID8agg, autophagy was significantly induced during serum starvation in PD-L1^{lo} B16 (Fig. 3D), the appropriate physiologic response. Consistent with Western blot data, there were more LC3 foci in PD-L1^{lo} B16 cells indicative of higher autophagosome formation versus control B16 under basal conditions and serum starvation (Fig. 3E), consistent with tumor cell PD-L1-mediated suppression of autophagy in B16.

PD-L1 sensitizes tumor cells to autophagy inhibitors *in vitro*

Because PD-L1 depletion deregulates autophagy, including cell-specific effects (Fig. 3B–E), we tested effects of the pharmacological autophagy inhibitor chloroquine (18,19). In contrast to basal PD-L1 proliferation effects, PD-L1^{lo} B16 cells were the most resistant to *in vitro* chloroquine-mediated proliferation inhibition, whereas PD-L1^{hi} cells were the most sensitive (Fig. 4A). Consistent with B16 cell data, PD-L1^{lo} ID8agg cells were significantly more resistant to chloroquine-mediated proliferation inhibition versus control ID8agg cells (Fig. 4A). Using the autophagy inhibitor 3-methyladenine (20), similar, but less pronounced proliferation effects were seen in both B16 and ID8agg cells (data not shown).

PD-L1 sensitizes B16 but not ID8agg cells to pharmacologic autophagy inhibitors *in vivo*

Consistent with *in vitro* data, chloroquine and 3-methyladenine were significantly more effective in reducing control versus PD-L1^{lo} B16 challenge into WT mice (Fig. 4B–D). Because autophagy inhibitors could also affect anti-tumor immunity, we assessed effects in T cell-deficient βδ TCR KO mice, where chloroquine retained its clinically activity against

control B16 (Fig. 4E) and remained ineffective against PD-L1^{lo} (Fig. 4F). Similarly, in NSG mice, chloroquine was significantly effective against challenge with control B16 cells (Fig. 4G), but was ineffective in reducing tumor growth in mice challenged with PD-L1^{lo} B16 cells (Fig. 4H). Together, these data support the concept that tumor PD-L1 sensitizes B16 melanoma to autophagy inhibitors independent of T cell immunity, and that tumor PD-L1 expression predicts autophagy-dependent growth. Consistent with dependence on autophagy that modulates cellular stress, serum starvation, which inhibits mTOR signaling and constrains cell dependence on autophagy, significantly reduced PD-L1^{hi} and control B16 cell viability *in vitro* under serum starvation conditions (with greatest effect in PD-L1^{hi} cells). We found reduced but significant effects in parental B16, and negligible effects in PD-L1^{lo} cells (Fig. 4I). By contrast, neither chloroquine nor 3-methyladenine improved survival against control or PD-L1^{lo} ID8agg challenge *in vivo* (Fig 4J). These data further establish common and cell-specific PD-L1 signaling effects.

Tumor PD-L1 regulates tumor mTOR signals

mTOR is a serine/threonine kinase regulating cellular growth and metabolism that is elevated in many cancers (26,27) and recently shown to be affected by tumor-intrinsic PD-L1 (11,15). As mTOR regulates important cellular processes including autophagy through distinct mTORC1 and mTORC2 complexes with distinct functions (28), we assessed additional mTOR signaling details. ID8agg RNA-seq identified potential mTOR signaling effects of PD-L1 (Table 1, bottom). For example, the mTORC1 activator *Rheb1* was significantly lower in PD-L1^{lo} cells ($p=5.35x10^{-7}$), consistent with reduced mTORC1 signaling. *Prps6,* a translation regulator controlled by mTORC1 was also significantly reduced ($p=7.97x10^{-7}$). mTORC2 activity is defined by target phosphorylation and cannot be assessed this way.

Tumor PD-L1 regulates mTOR distinctly during serum starvation and treatment and in distinct tumors

We used immunoblots to validate that tumor PD-L1 promotes basal mTORC1 signaling as assessed by P70S6K^{T389} phosphorylation (Fig. 5A,B). PD-L1^{lo} ID8agg cells paradoxically increased mTORC1 during serum starvation whereas PD-L1^{lo} B16 cells did not (Fig. 5A,B). Rapamycin effectively suppressed mTORC1 in control B16 and ID8agg cells as expected and equally suppressed mTORC1 in PD-L1^{lo} B16 and ID8agg cells (Fig. 5D, Suppl. Fig. 6). PD-L1^{lo} B16 and ID8agg cells were more sensitive to rapamycin-mediated suppression of proliferation *in vitro* versus control cells, by MTT assay (Fig. 5C), suggesting that PD-L1 regulation of metabolic activity is mTORC1-dependent, although mTORC2 effects cannot be excluded (29,30). Under basal conditions PD-L1 inhibited phosphorylation of the mTORC2 substrate Akt^{S473} in B16 and ID8agg (Fig. 5A,B), consistent with reduced mTORC2 activity (31–33). Rapamycin differentially affected Akt^{S473} phosphorylation in B16 versus ID8agg in a PD-L1-dependent manner (Fig. 5D). mTORC1 and phosphorylated P70S6K^{T389} can mediate a negative feedback loop on phosphoinositide 3-kinase (PI3K)/Akt (34,35) which is de-repressed by rapamycin. Hence, rapamycin effects on Akt^{S473} phosphorylation could be mTORC2-independent.

We next treated cells with chloroquine to inhibit autophagy and found that it inhibited mTORC1 as expected (36,37) in control ID8agg but paradoxically increased mTORC1 in control B16 cells. Chloroquine had no effect on mTORC1 in PD-L1^{lo} ID8agg cells but significantly increased mTORC1 in PD-L1^{lo} B16 cells (Suppl. Fig. 6). Nonetheless, no observed mTOR effects readily explain how PD-L1 sensitizes cells to chloroquine-mediated cell proliferation inhibition. Thus, PD-L1-mediated mTOR and autophagy effects could be independent. Other effects of chloroquine or rapamycin or their combination varied between the two tumors based on basal versus serum starvation conditions and PD-L1 status (Fig. 5D, Suppl. Fig. 6 and much additional data not shown), likely reflecting distinct tumor mutational landscapes in ovarian cancer (38) versus melanoma (39) and further supporting common versus cell-specific PD-L1 signaling effects. As mTOR and autophagy regulate responses to cytotoxic insults including chemotherapy and cytokines (40,41), we explored additional effects. Tumor PD-L1 rendered B16 cells resistant to tumor necrosis factor (TNF)-α *in vitro* whereas ID8agg cells were intrinsically more resistant and PD-L1 had no effect on TNF-α-mediated cytotoxicity (Suppl. Fig. 7A). Surprisingly, tumor PD-L1 did not significantly alter sensitivity of B16 or ID8agg to the cytotoxic agents cisplatin or paclitaxel (Suppl. Fig. 7B–C). Thus, tumor PD-L1 is a pro-survival agent, but effects depend on the specific toxic insult.

Cell-intrinsic PD-L1 regulates proliferation, mTOR signaling, and autophagy in human ovarian cancer cells

To test human relevance, we first showed that the human ES2 ovarian cancer cell line expressed basal PD-L1, and then engineered PD-L1^{lo} ES2 cells (Fig. 6A,B). Some ES2 cells also express basal PD-1 (Fig. 6B). Consistent with B16 and ID8agg data, PD-L1^{lo} ES2 cells proliferated significantly slower than control ES2 (Fig. 6C). LC3-II versus LC3-I was increased in PD-L1^{lo} but not in control cells (Fig. 6D), consistent with increased autophagic flux when PD-L1 was reduced. In support, LC3 foci were reduced in control versus PD-L1^{lo} cells indicative of PD-L1-mediated decrease in autophagosome formation (Fig. 6E). Altogether these data are consistent with PD-L1-dependent suppression of autophagic flux in human cancer cells, similar to mouse cell data. Further consistent with B16 and ID8agg data, PD-L1 in ES2 cells augmented mTORC1 signals (P70S6K^{T389} phosphorylation). By contrast to B16 and ID8agg data, PD-L1 knock down eliminated ES2 mTORC2 activation (Akt^{S473} phosphorylation) (Fig. 6F).

Validating our observations in B16 and ID8agg, control ES2 cells were significantly more sensitive to proliferation inhibition by chloroquine compared to PD-L1^{lo} ES2 cells (Fig. 6G), further suggesting that PD-L1 regulation of cancer cell autophagy and autophagy dependence could be a common mechanism in PD-L1 expressing mouse and human cancer cells.

Discussion

Tumor-expressed PD-L1 alters tumor immunopathogenesis by delivering negative signals to PD-1-expressing anti-tumor T cells (3–7), but emerging evidence shows that PD-L1 and PD-1 also have tumor-intrinsic functions (11,15). Our work now clearly establishes that

tumor intrinsic PD-L1 has additional, important tumor intrinsic effects. We found that tumor PD-L1 promoted cell-intrinsic growth in two distinct tumor types (melanoma and ovarian cancer), in distinct anatomic compartments (skin and peritoneum) and in an immune-independent fashion for both. Thus, these properties are not specific to one single cell type or anatomic location.

αPD-L1 can alter PD-L1-mediated cell-intrinsic growth signals as α-PD-L1 slowed B16 tumor growth in NSG mice incapable of mediating tumor-specific immunity or antibody-dependent cellular cytotoxicity. Melanoma PD-L1 promoted immune-independent *bona fide* metastases from subcutaneous melanoma, a more stringent model than intravenous cell challenge. Increased tumor growth and proliferation likely contributes to increased metastases, but additional factors could also contribute. Further work is needed to understand applicability to additional cancers and define mechanisms.

αPD-1 and αPD-L1 comparably inhibited B16 growth *in vitro, and* comparably reduced B16 metastases *in vivo*. These data are consistent with tumor PD-L1/tumor PD-1 cooperation as only ~5–10% of cells expressed PD-1. *In vivo*, αPD-L1 effects appears to be directed to tumor and not other PD-L1-expressing cells as αPD-L1: i) had no significant effect on PD-L1^{lo} B16 melanoma growth in WT mice, and ii) was fully protective in PD-L1 KO mice challenged with parental B16 cells. However, this treatment effect could be tumor- or compartment-specific, as αPD-L1 did not slow tumor growth or improve survival in intraperitoneal ID8agg ovarian cancer challenged NSG mice, despite reducing *in vitro* proliferation. In support of tumor-specific effects, a recent report showed that αPD-L1 did not slow PD-L1^{+} sarcoma growth in NSG mice (11). Specific tumors might be refractory to PD-L1-driven growth or survival signals owing to tumor-specific mutations (38,39), degree of PD-L1 expression, antibody affinity and delivery differences, or other factors.

Tumor PD-L1 suppressed tumor autophagy in melanoma and ovarian cancer, suggesting that autophagy disruption could be a relatively general tumor PD-L1 effect. Tumor PD-L1 regulates glucose metabolism in sarcomas (11), suggesting that PD-L1 could have a variety of important cell-intrinsic metabolic effects. Furthermore, B7-H3 regulates glucose metabolism in breast cancer cells (42) suggesting that the B7-H superfamily to which PD-L1 and B7-H3 belong (43) or the immunoglobulin superfamily to which these and PD-1 all belong (13), could have important tumor metabolic effects, which is an area meriting additional investigations. Our RNA-seq data demonstrated numerous potentially PD-L1-regulated genes. Ingenuity Pathway Analysis determined that many critical pathways were affected, including immune cell trafficking (chemokines and cytokines), inflammation, TGF-β signalling, metabolism and cancer stem cell genes among others (our unpublished data), in addition to effects shown here. Thus, much additional, important PD-L1-mediated tumor cell signalling likely awaits definition.

We found that PD-L1-replete B16 melanoma and ID8agg ovarian cancer cells exhibit low basal autophagy, with high mTORC1 activity, and were disproportionately sensitive to autophagy inhibitor-mediated growth reduction compared to cancer cells with low PD-L1 expression. We postulate that further autophagy reduction in cancer cells with elevated mTORC1 activity and low autophagic activity (directly related to PD-L1 expression), is

catastrophic. In support, autophagy levels can be fine-tuned to allow cells to meet metabolic demands (44) without compromising other functions. *In vivo,* this PD-L1-mediated balance augments clinical response to autophagy inhibitors. These data suggest that autophagy inhibitors could boost αPD-L1 treatment of PD-L1 positive cancers. Despite high levels of autophagic flux, PD-L1^{lo} tumor cells might have a reduced autophagy requirement due to lower metabolic demand and/or cellular stress, as supported by reduced sensitivity to autophagy inhibitors. Furthermore, pharmacologic inhibitors could incompletely inhibit this high autophagy for clinical effect. Genetic approaches to autophagy manipulation are required to explore mechanisms further, but our data support the thesis that tumor PD-L1 expression and basal autophagy levels could be a biomarker for effective clinical autophagy inhibitor use. Our data also suggest that autophagy inhibition plus αPD-L1 merits clinical investigation.

As autophagy is a tumor survival mechanism, we expected that tumor PD-L1 could affect cell viability after specific insults, and found differences in survival in serum starvation, mTOR and autophagy inhibitors and TNF-α. Surprisingly, though, we did not detect a difference in sensitivity to cis-platinum or paclitaxel *in vitro*. An abstract suggested that tumor PD-L1 protects from cytotoxic chemotherapy (10). That work used PD-L1 overexpression and did not specify cell lines or cytotoxic agents, making us unable to comment on potential differences from that work.

PD-L1 regulates tumor mTOR signals in melanoma and sarcoma (11,15), but mechanistic details are lacking, and unreported in ovarian cancer. We show that low PD-L1 in melanoma and ovarian cancer cells results in reduced phosphorylation of the mTORC1 substrate P70S6K^{T389}. PD-L1^{lo} cells proliferated more slowly than control lines, suggesting that lower mTORC1 activity in PD-L1^{lo} cells compromises their growth. Proliferation inhibition by the (predominantly) mTORC1 inhibitor rapamycin abolished P70S6K^{T389} phosphorylation in control and PD-L1^{lo} B16 and ID8agg cells *in vitro* as expected, yet PD-L1^{lo} cells were more rapamycin-sensitive than control cells, suggesting that proliferation of PD-L1^{lo} tumors is more dependent on basal mTORC1 activity compared to PD-L1-replete tumor cells. PD-L1-mediated mTORC1 effects could differ in tumor cell metabolism, survival and therapeutic outcomes. Nonetheless, these data support the concept that tumor PD-L1-dependent mTORC1 activity drives proliferation. Thus, PD-L1 expression could predict mTORC1 activity and rapamycin-sensitive tumor growth, which is clinically exploitable. For instance, these data suggest that αPD-L1 and/or αPD-1 immunotherapies combined with mTOR inhibitors in treating PD-1/PD-L1-replete tumors, or mTOR inhibitors alone in treating PD-1^{lo}/PD-L1^{lo} tumors are rational approaches.

Other mTORC1 substrates, mTORC2 or other rapamycin effects could also mediate specific PD-L1-dependent effects. For example, mTORC2 and its substrate Akt drive tumor cell growth and survival (45). We found that phosphorylation of the mTORC2 substrate Akt^{S473} was induced in PD-L1^{lo} B16 and ID8agg cells. In contrast to parental ID8agg cells, rapamycin did not further induce pAkt^{S473} in PD-L1^{lo} cells, demonstrating a PD-L1-dependent effect, perhaps from low basal mTORC1 and P70S6K activities, in which case negative feedback on Akt could be inactive and thus unaffected by rapamycin. We speculate that PD-L1-driven mTORC1 activation accounts for reduced autophagy, but genetic and

additional approaches are required for definitive mechanistic insights. Additional study of PD-L1-mediated mTOR signalling and outcomes of mTOR inhibition (*e.g.* metabolic activity), and cell-specific effects could help optimize mTOR inhibition strategies to treat selected cancers. As PD-L1, PD-1 and B7-H3 all regulate tumor mTOR signaling (11,15,42), this could be another general feature of selected immunoglobulin superfamily members and requires additional study.

Finally, we demonstrated human relevance by showing that cell-intrinsic PD-L1 in the human ES2 ovarian cancer cell line controls proliferation, mTORC1, autophagic flux and sensitivity to autophagy inhibitors. PD-L1 in human melanoma cells controls PD-1 effects on melanoma growth and mTOR signals (15). Thus, human studies merit much additional attention.

In summary, we show that tumor cell-intrinsic PD-L1 signals mediate effects common to melanoma and ovarian cancer cells in mouse lines, and effects extend to human ovarian cancer cells. PD-L1 promotes tumor cell proliferation and immune-independent growth in melanoma and ovarian cancer cells, and metastatic melanoma spread *in vivo*. Tumor cell-intrinsic PD-L1 altered autophagy inhibitor and mTOR inhibitor efficacy. PD-L1 promoted basal mTORC1 activation in all cells tested, and inhibited phosphorylation of the mTORC2 substrate Akt in mouse lines but not the human line tested. αPD-L1 inhibited *in vivo* melanoma growth but not ovarian cancer growth in an immune-independent fashion, and melanoma but not ovarian cancer cells were slowed by autophagy inhibitors *in vivo.* Thus, tumor PD-L1 could be a biomarker for response to mTOR or autophagy inhibitors in selected cancers. Tumor PD-L1 appeared to cooperate with tumor PD-1 for selected effects. As our understanding of tumor cell-intrinsic PD-L1 effects increases, our ability to predict treatment responses to various agents and combine them in rationale ways for more effective clinical use will improve. Given the extraordinary effect that PD-L1 appears to have on diverse, critical cellular processes, much additional work in this area is merited.

Supplementary Material

Refer to Web version on PubMed Central for supplementary material.

Acknowledgments

Financial support: T. Curiel (CA170491, CA54174, CA054174, CDMRP, The Holly Beach Public Library, The Owens Foundation and the Skinner endowment). K. Thedieck (Rosalind Franklin Fellowship, BMBF e:Med Young investigator network GlioPATH (01ZX1402B), BMBF e:Med Demonstrator project MAPTor-NET (31P9013A), Ubbo Emmius Funds, Stichting Michelle). M.J. Turk (CA120777), C. Clark (CA206398, UTHSCSA MD/PhD Program).

Work was supported by grants from the NIH, European governments and private foundations.

References

1. Zou W, Chen L. Inhibitory B7-family molecules in the tumour microenvironment. Nat Rev Immunol. 2008; 8(6):467–77. [PubMed: 18500231]
2. Paterson AM, Brown KE, Keir ME, Vanguri VK, Riella LV, Chandraker A, et al. The programmed death-1 ligand 1:b7-1 pathway restrains diabetogenic effector T cells in vivo. J Immunol. 2011; 187(3):1097–105. [PubMed: 21697456]

3. Topalian SL, Drake CG, Pardoll DM. Targeting the PD-1/B7-H1(PD-L1) pathway to activate anti-tumor immunity. Curr Opin Immunol. 2012; 24(2):207–12. [PubMed: 22236695]

4. Dong H, Strome SE, Salomao DR, Tamura H, Hirano F, Flies DB, et al. Tumor-associated B7-H1 promotes T-cell apoptosis: A potential mechanism of immune evasion. Nat Med. 2002; 8(8):793–800. [PubMed: 12091876]

5. Brahmer JR, Tykodi SS, Chow LQ, Hwu WJ, Topalian SL, Hwu P, et al. Safety and activity of anti-PD-L1 antibody in patients with advanced cancer. N Engl J Med. 2012; 366(26):2455–65. [PubMed: 22658128]

6. Taube JM, Anders RA, Young GD, Xu H, Sharma R, McMiller TL, et al. Colocalization of inflammatory response with B7-h1 expression in human melanocytic lesions supports an adaptive resistance mechanism of immune escape. Sci Transl Med. 2012; 4(127):127ra37.

7. Pardoll DM. The blockade of immune checkpoints in cancer immunotherapy. Nat Rev Cancer. 2012; 12(4):252–64. [PubMed: 22437870]

8. Topalian SL, Hodi FS, Brahmer JR, Gettinger SN, Smith DC, McDermott DF, et al. Safety, activity, and immune correlates of anti-PD-1 antibody in cancer. N Engl J Med. 2012; 366(26):2443–54. [PubMed: 22658127]

9. Azuma T, Yao S, Zhu G, Flies AS, Flies SJ, Chen L. B7-H1 is a ubiquitous antiapoptotic receptor on cancer cells. Blood. 2008; 111(7):3635–43. [PubMed: 18223165]

10. Orzechowski A, Dong H. B7-H1 confers tumor chemoresistance by regulating MAPK/ERK activation. Cancer Research. 2014; 74(74) abstract 5026.

11. Chang CH, Qiu J, O'Sullivan D, Buck MD, Noguchi T, Curtis JD, et al. Metabolic Competition in the Tumor Microenvironment Is a Driver of Cancer Progression. Cell. 2015; 162(6):1229–41. [PubMed: 26321679]

12. Mahalingam D, Mita M, Sarantopoulos J, Wood L, Amaravadi RK, Davis LE, et al. Combined autophagy and HDAC inhibition: a phase I safety, tolerability, pharmacokinetic, and pharmacodynamic analysis of hydroxychloroquine in combination with the HDAC inhibitor vorinostat in patients with advanced solid tumors. Autophagy. 2014; 10(8):1403–14. [PubMed: 24991835]

13. Wang S, Bajorath J, Flies DB, Dong H, Honjo T, Chen L. Molecular Modeling and Functional Mapping of B7-H1 and B7-DC Uncouple Costimulatory Function from PD-1 Interaction. J Exp Med. 2003; 197(9):1083–91. [PubMed: 12719480]

14. Jiang B, Liu F, Liu Z, Zhang T, Hua D. B7-H3 increases thymidylate synthase expression via the PI3k-Akt pathway. Tumour biology : the journal of the International Society for Oncodevelopmental Biology and Medicine. 2016

15. Kleffel S, Posch C, Barthel SR, Mueller H, Schlapbach C, Guenova E, et al. Melanoma Cell-Intrinsic PD-1 Receptor Functions Promote Tumor Growth. Cell. 2015; 162(6):1242–56. [PubMed: 26359984]

16. Lin PY, Sun L, Thibodeaux SR, Ludwig SM, Vadlamudi RK, Hurez VJ, et al. B7-H1-Dependent Sex-Related Differences in Tumor Immunity and Immunotherapy Responses. J Immunol. 2010; 185(5):2747–53. [PubMed: 20686128]

17. Facciabene A, Peng X, Hagemann IS, Balint K, Barchetti A, Wang LP, et al. Tumour hypoxia promotes tolerance and angiogenesis via CCL28 and T(reg) cells. Nature. 2011; 475(7355):226–30. [PubMed: 21753853]

18. Xie X, White EP, Mehnert JM. Coordinate autophagy and mTOR pathway inhibition enhances cell death in melanoma. PloS one. 2013; 8(1):e55096. [PubMed: 23383069]

19. Maes H, Kuchnio A, Peric A, Moens S, Nys K, De Bock K, et al. Tumor vessel normalization by chloroquine independent of autophagy. Cancer Cell. 2014; 26(2):190–206. [PubMed: 25117709]

20. Li J, Yang D, Wang W, Piao S, Zhou J, Saiyin W, et al. Inhibition of autophagy by 3-MA enhances IL-24-induced apoptosis in human oral squamous cell carcinoma cells. J Exp Clin Cancer Res. 2015; 34:97. [PubMed: 26361755]

21. Curiel TJ, Wei S, Dong H, Alvarez X, Cheng P, Mottram P, et al. Blockade of B7-H1 improves myeloid dendritic cell-mediated antitumor immunity. Nat Med. 2003; 9(5):562–7. [PubMed: 12704383]

22. Schneider CA, Rasband WS, Eliceiri KW. NIH Image to ImageJ: 25 years of image analysis. Nature methods. 2012; 9(7):671–5. [PubMed: 22930834]
23. Pedersen SR, Sorensen MR, Buus S, Christensen JP, Thomsen AR. Comparison of vaccine-induced effector CD8 T cell responses directed against self- and non-self-tumor antigens: implications for cancer immunotherapy. J Immunol. 2013; 191(7):3955–67. [PubMed: 24018273]
24. Roby KF, Taylor CC, Sweetwood JP, Cheng Y, Pace JL, Tawfik O, et al. Development of a syngeneic mouse model for events related to ovarian cancer. Carcinogenesis. 2000; 21(4):585–91. [PubMed: 10753190]
25. Pampliega O, Orhon I, Patel B, Sridhar S, Diaz-Carretero A, Beau I, et al. Functional interaction between autophagy and ciliogenesis. Nature. 2013; 502(7470):194–200. [PubMed: 24089209]
26. Riaz H, Riaz T, Hussain SA. mTOR inhibitors: A novel class of anti-cancer agents. Infectious agents and cancer. 2012; 7(1):1. [PubMed: 22214493]
27. Guertin DA, Sabatini DM. Defining the role of mTOR in cancer. Cancer cell. 2007; 12(1):9–22. [PubMed: 17613433]
28. Dao V, Pandeswara S, Liu Y, Hurez V, Dodds S, Callaway D, et al. Prevention of carcinogen and inflammation-induced dermal cancer by oral rapamycin includes reducing genetic damage. Cancer Prev Res (Phila). 2015; 8(5):400–9. [PubMed: 25736275]
29. Sarbassov DD, Ali SM, Sengupta S, Sheen JH, Hsu PP, Bagley AF, et al. Prolonged rapamycin treatment inhibits mTORC2 assembly and Akt/PKB. Molecular cell. 2006; 22(2):159–68. [PubMed: 16603397]
30. Lamming DW, Ye L, Katajisto P, Goncalves MD, Saitoh M, Stevens DM, et al. Rapamycin-induced insulin resistance is mediated by mTORC2 loss and uncoupled from longevity. Science. 2012; 335(6076):1638–43. [PubMed: 22461615]
31. Sarbassov DD, Guertin DA, Ali SM, Sabatini DM. Phosphorylation and regulation of Akt/PKB by the rictor-mTOR complex. Science. 2005; 307(5712):1098–101. [PubMed: 15718470]
32. Hresko RC, Mueckler M. mTOR. RICTOR is the Ser473 kinase for Akt/protein kinase B in 3T3-L1 adipocytes. The Journal of biological chemistry. 2005; 280(49):40406–16. [PubMed: 16221682]
33. Jacinto E, Facchinetti V, Liu D, Soto N, Wei S, Jung SY, et al. SIN1/MIP1 maintains rictor-mTOR complex integrity and regulates Akt phosphorylation and substrate specificity. Cell. 2006; 127(1): 125–37. [PubMed: 16962653]
34. Hsu PP, Kang SA, Rameseder J, Zhang Y, Ottina KA, Lim D, et al. The mTOR-regulated phosphoproteome reveals a mechanism of mTORC1-mediated inhibition of growth factor signaling. Science. 2011; 332(6035):1317–22. [PubMed: 21659604]
35. Yu Y, Yoon SO, Poulogiannis G, Yang Q, Ma XM, Villen J, et al. Phosphoproteomic analysis identifies Grb10 as an mTORC1 substrate that negatively regulates insulin signaling. Science. 2011; 332(6035):1322–6. [PubMed: 21659605]
36. Settembre C, Zoncu R, Medina DL, Vetrini F, Erdin S, Huynh T, et al. A lysosome-to-nucleus signalling mechanism senses and regulates the lysosome via mTOR and TFEB. The EMBO journal. 2012; 31(5):1095–108. [PubMed: 22343943]
37. Zoncu R, Bar-Peled L, Efeyan A, Wang S, Sancak Y, Sabatini DM. mTORC1 senses lysosomal amino acids through an inside-out mechanism that requires the vacuolar H(+)-ATPase. Science. 2011; 334(6056):678–83. [PubMed: 22053050]
38. Westcott PM, Halliwill KD, To MD, Rashid M, Rust AG, Keane TM, et al. The mutational landscapes of genetic and chemical models of Kras-driven lung cancer. Nature. 2015; 517(7535): 489–92. [PubMed: 25363767]
39. Spranger S, Bao R, Gajewski TF. Melanoma-intrinsic beta-catenin signalling prevents anti-tumour immunity. Nature. 2015
40. Zoncu R, Efeyan A, Sabatini DM. mTOR: from growth signal integration to cancer, diabetes and ageing. Nat Rev Mol Cell Biol. 2010; 12(1):21–35. [PubMed: 21157483]
41. Baginska J, Viry E, Berchem G, Poli A, Noman MZ, van Moer K, et al. Granzyme B degradation by autophagy decreases tumor cell susceptibility to natural killer-mediated lysis under hypoxia. Proc Natl Acad Sci U S A. 2013; 110(43):17450–5. [PubMed: 24101526]

42. Nunes-Xavier CE, Karlsen KF, Tekle C, Pedersen C, Oyjord T, Hongisto V, et al. Decreased expression of B7-H3 reduces the glycolytic capacity and sensitizes breast cancer cells to AKT/mTOR inhibitors. Oncotarget. 2016

43. Chapoval AI, Ni J, Lau JS, Wilcox RA, Flies DB, Liu D, et al. B7-H3: a costimulatory molecule for T cell activation and IFN-gamma production. Nat Immunol. 2001; 2(3):269–74. [PubMed: 11224528]

44. Kaur J, Debnath J. Autophagy at the crossroads of catabolism and anabolism. Nature reviews Molecular cell biology. 2015; 16(8):461–72. [PubMed: 26177004]

45. Laplante M, Sabatini DM. mTOR signaling in growth control and disease. Cell. 2012; 149(2):274–93. [PubMed: 22500797]

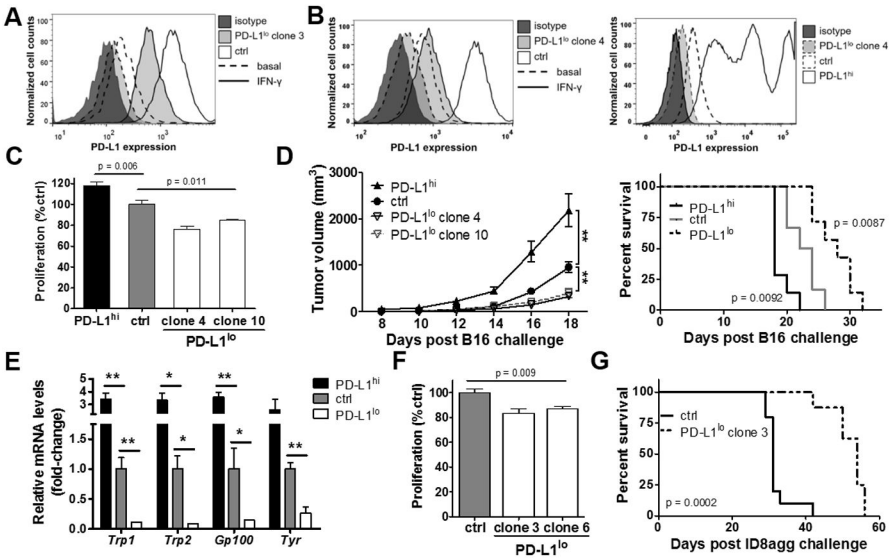

Figure 1. Tumor-intrinsic PD-L1 controls immune-independent growth and metastatic spread

Flow cytometry for PD-L1 expression of *in vitro* cultured cells. Interferon (IFN)-γ 0.1 ng/mL added for 48 h as indicated for (**A**) ID8agg or (**B**) B16**. C.** Proliferation *in vitro* of B16 cells determined by MTT versus control (ctrl, set at 100%). p-value, unpaired *t* test. **D.** NSG mice challenged subcutaneously with indicated B16 cells. P values for tumor size by two-way ANOVA and for survival by log-rank test. **E.** NSG mice challenged with indicated B16 cells and sacrificed on day 18. Genes in whole lung lysates by qPCR. p-value, unpaired *t* test. *, $p < 0.05$, **, $p < 0.01$. **F.** Proliferation *in vitro* of ID8agg cells as in panel **C** and survival *in vivo* (**G**) as in panel **D** after intraperitoneal ID8agg challenge.

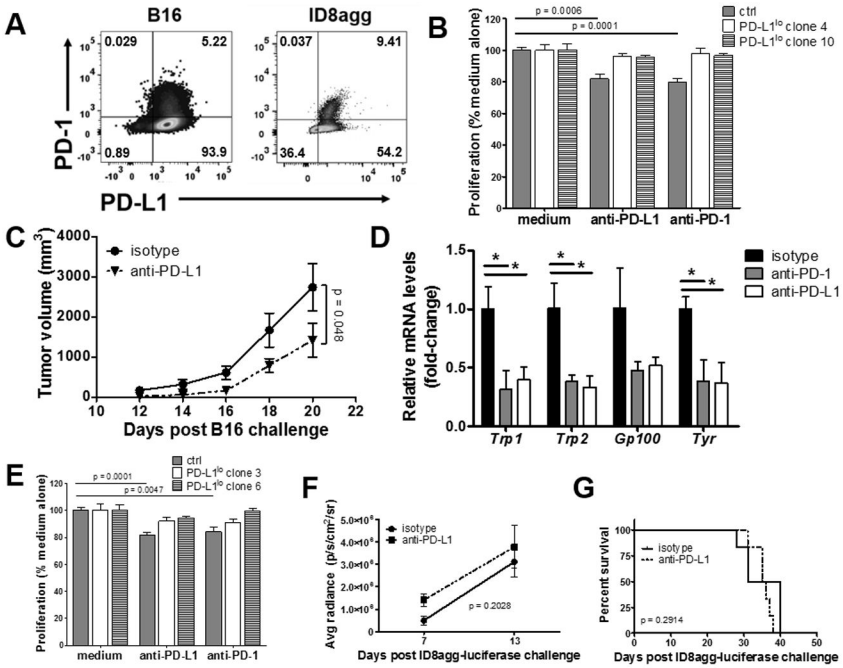

Figure 2. αPD-L1 reduces B16 growth and metastatic spread in NSG mice

A. PD-1 and PD-L1 expression in B16 melanoma and ID8agg ovarian cells measured by flow cytometry. **B.** Proliferation *in vitro* of B16 cells ± αPD-L1 or αPD-1 (50 μg/mL each) determined by MTT versus control (ctrl, set at 100%). p-value, unpaired *t* test. **C.** NSG mice challenged with indicated B16 cells and treated with αPD-L1 200 μg every other day starting one day following challenge. p-value, two-way ANOVA. **D.** qPCR for indicated genes from whole lung lysates from mouse challenged as in **C,** given αPD-L1 or αPD-1 200 μg every other day starting on day following challenge, day 18. Unpaired *t* test. *, $p < 0.05$, **, $p < 0.01$. **E.** Proliferation *in vitro* of ID8agg cells treated as in **B.** NSG mice challenged with ID8agg-luciferase and treated with αPD-L1 200 μg every other day starting one day following challenge. P values for average luciferase radiance (**F**) by two-way ANOVA and for survival (**G**) by log-rank test.

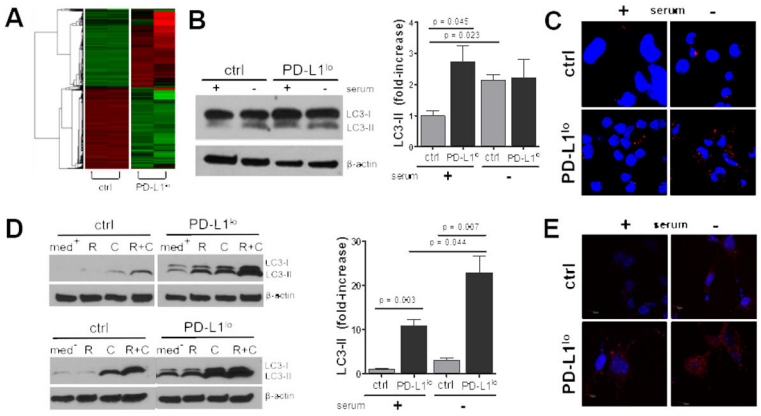

Figure 3. PD-L1 regulates tumor autophagy genes and functions

A. RNA was isolated from *in vitro* cultured control or PD-L1^{lo} ID8agg cells and global genes were assessed using David Bioinformatics. 5.8E-10, 5.8 x 10^{-10}, *etc*. **B.** Western blot of lysed ID8agg cells from basal (+) or serum starved (−) (24 h) conditions (left). Right, summary data of three independent experiments. p-values, unpaired *t* test. **C.** Confocal images of autophagosome formation by LC-3 aggregation (red) in control versus PD-L1^{lo} ID8agg under basal or serum starved (24 h) conditions. Blue, DAPI for nuclei. **D.** Analyses of B16 cells as in **B**, (med + or − for basal and serum starved conditions, respectively) treated with rapamycin (R) for 16 h, chloroquine (C) for 6 h or both**. E.** Confocal images of autophagosome formation for control versus PD-L1^{lo} B16 as in **C**.

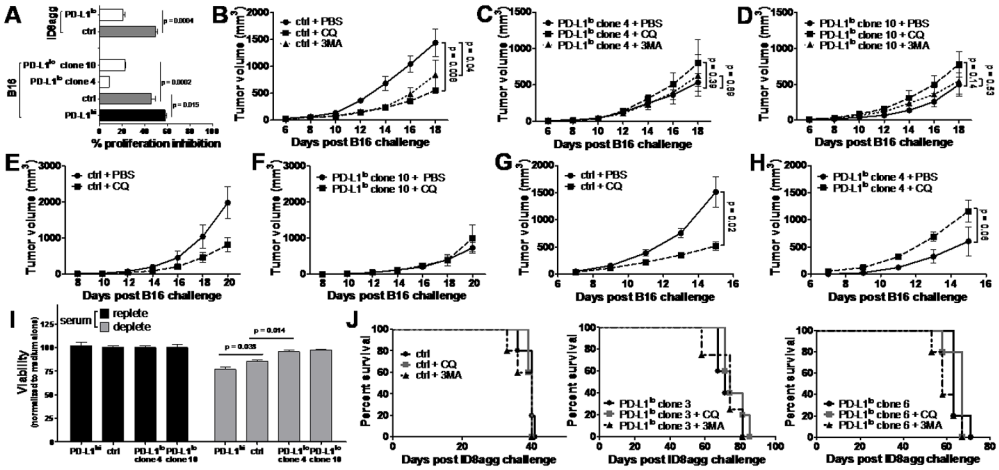

Figure 4. Tumor PD-L1 regulates response to pharmacologic autophagy inhibitors

A. Indicated cells were cultured with 50 μM chloroquine and proliferation inhibition (100%-% proliferation by MTT, with control set at 0%) assessed 72 h later. P values from unpaired *t* test. **B-D,** wild type mice challenged with indicated cells and treated with chloroquine (CQ) or 3-methyladenine (3MA) as described in Materials and Methods. p-values, two-way ANOVA. PBS, phosphate buffered saline control. **E-F**. βδ TCR KO mice challenged and treated as in **B-D. G-H.** NSG mice challenged and treated as in **B-D. I.** Indicated B16 cells from basal (+) or serum starved (−) (24 h) conditions and cell viability normalized to basal controls assessed on a Vi-Cell. P values from unpaired *t* test. **J.** WT females challenged with indicated ID8agg, 4 x 10^6 cells intraperitoneally, and treated with chloroquine or 3MA as in panels **B-D**. No differences are significant.

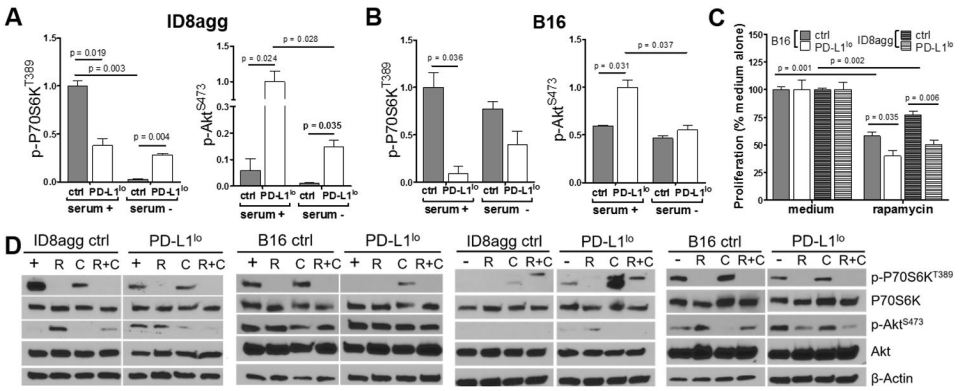

Fig. 5. Tumor PD-L1 regulates mTOR distinctly and blunts rapamycin proliferation inhibition

Summary data of Western blots for P70S6K^{T389} and Akt^{S473} phosphorylation as ratios of phospho-protein to total protein under basal or serum starved (24 h) conditions for ID8agg (**A**) and B16 (**B**) cells. Statistical analyses from average of three independent experiments. **C.** Indicated cells were cultured with 5 nM rapamycin and proliferation by MTT, with control set at 100% assessed 72 h later. **D.** Representative Western blots for treatments with rapamycin (R) for 16 h, chloroquine (C) for 6 h or both (R+C) under basal (+) conditions for under serum-starved (−) conditions for ID8agg and B16. Summary data for these blots are in Supplemental Fig. 6.

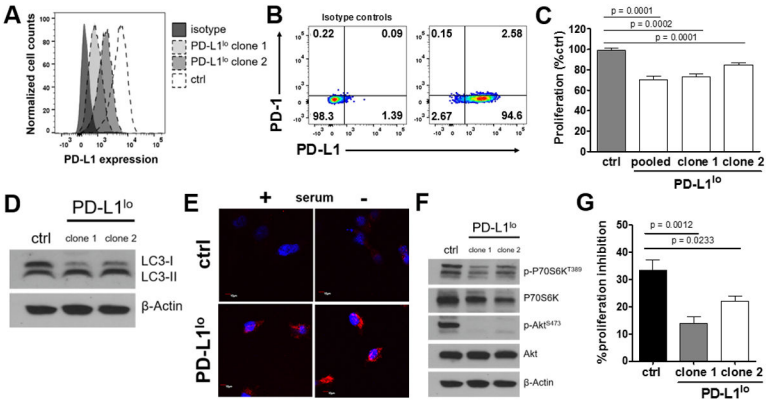

Fig. 6. Tumor cell-intrinsic PD-L1 regulates proliferation, mTOR signaling, and autophagy in human ovarian cancer cells

A. Flow cytometry for PD-L1 expression of *in vitro* cultured ES2 human ovarian cancer cells showing PD-L1 knock-down by shRNA. **B.** PD-1 and PD-L1 expression by flow cytometry. **C.** Proliferation *in vitro* of ES2 cells determined by MTT versus control (ctrl, set at 100%). p-value, unpaired *t* test. **D.** Western blot for LC3I/II in ES2 cell lysates from basal conditions. **E.** Confocal images of autophagosome formation by LC-3 aggregation (red) in control versus PD-L1^{lo} ES2 under basal or serum starved (24 h) conditions. Blue, DAPI for nuclei. **F.** Western blot for P70S6K^{T389} and Akt^{S473} phosphorylation in ES2 cells under basal conditions. **G.** Control and PD-L1^{lo} ES2 cells were cultured with 50 μM chloroquine and proliferation inhibition (100%-% proliferation by MTT, with control set at 0%) assessed 72 h later. P-values, unpaired *t* test.

Table 1

Selected genes from RNA-seq analyses of control and PD-L1l^{o} ID8agg, as ratio of gene expression in PD-L1^{lo} versus control cells. **Top**, autophagy pathway genes. **Bottom**, mTOR pathway signaling genes.

	Gene	Fold-change (PD-L1^{lo}/ctrl)	P value
Autophagy	*Ire1a*	2.58	5.8E-10
	Atg9b	−2.46	7.7E-08
	Atg2a	−1.79	6.5E-04
	Perk	−1.65	2.6E-03
	Atg7	−1.69	6.7E-03
	Atf4	1.41	3.9E-02
	Atg12	1.43	6.1E-02
	Atg13	−1.42	7.5E-02

	Gene	Fold-change (PD-L1^{lo}/ctrl)	P value
mTOR	*Prkg2*	2.69	3.0E-10
	Pik3cd	−3.27	3.3E-09
	Irs1	2.81	1.4E-08
	Map3k6	−2.75	1.9E-08
	Rhebl1	−2.95	5.4E-07
	Rps6ka2	−3.32	8.0E-07
	Atp5k	−2.05	2.1E-05
	Rps6kl1	−8.81	5.0E-05
	Pdk4	−2.05	1.4E-03
	Map2k6	−2.35	1.4E-03